cross section (Fig. 2) decreases monotonically with energy. Thus, the maximum in the forward differential cross section seen from combining the data of Turkot, Collins, and Fujii and Cocconi et al. is caused by the energy dependence of the angular distribution and is not indicative of any maximum in the total cross section.

The narrow width of the peak at $\cos\theta = -1$ above 2.0 BeV suggests a peripheral interaction such as a one-nucleon exchange.[1] The energy dependence of $d\sigma/d\Omega$ near 90°, coupled with the smoothly varying angular distribution near 90°, is similar to the behavior observed in high-energy pp elastic scattering,[8] and thus is suggestive of a statistical interpretation.[9]

It is a pleasure to acknowledge the patience, skill, and diligence of J. Harris, W. Merkle, and the entire Cosmotron staff. The authors would also like to express their appreciation to the Brookhaven National Laboratory for its hospitality and assistance in this program.

*Work supported by Office of Naval Research and U. S. Atomic Energy Commission.

†National Science Foundation Predoctoral Fellow.

[1]M. L. Perl, L. W. Jones, and C. C. Ting, Phys. Rev. 132, 1273 (1963).

[2]J. Chahoud, G. Russo, and F. Selleri, Phys. Rev. Letters 11, 506 (1963).

[3]T. Yao, Phys. Rev. 134, B454 (1964).

[4]F. Turkot, G. B. Collins, and T. Fujii, Phys. Rev. Letters 11, 474 (1963).

[5]G. Cocconi, E. Lillethun, J. P. Scanlon, C. A. Stahlbrandt, C. C. Ting, J. Walters, and A. M. Wetherell, Phys. Letters 7, 222 (1963).

[6]B. Sechi-Zorn, Bull. Am. Phys. Soc. 7, 349 (1962).

[7]M. G. Mescheryakov, B. S. Neganov, N. P. Bogachev, and V. M. Sidorov, Dokl. Akad. Nauk SSSR 100, 673 (1955).

[8]G. Cocconi et al., Phys. Rev. Letters 11, 499 (1963); W. F. Baker et al., Phys. Rev. Letters 12, 132 (1964).

[9]G. Fast and R. Hagedorn, Nuovo Cimento 27, 856 (1963); G. Fast, R. Hagedorn, and L. W. Jones, Nuovo Cimento 27, 856 (1963); L. W. Jones, Phys. Letters 8, 287 (1964).

STUDY OF $S = -2$ BARYON SYSTEMS UP TO 2 BeV*

Gerald A. Smith, James S. Lindsey, Joseph J. Murray, Janice Button-Shafer, Angela Barbaro-Galtieri, Orin I. Dahl, Philippe Eberhard, William E. Humphrey, George R. Kalbfleisch, Ronald R. Ross, Frank T. Shively, and Robert D. Tripp

Department of Physics and Lawrence Radiation Laboratory, University of California, Berkeley, California

(Received 1 June 1964)

In this Letter we present evidence for existence of an 1810-MeV, $S = -2$ baryon state. During an extensive exposure of the 72-in. hydrogen bubble chamber to a separated beam of K^- at incident momenta of 2.45, 2.64, and 2.70 BeV/c, approximately 380 000 pictures have been taken, with 6 to 7 K^-'s and 1 to 2 π^-'s per picture. The 2.64- and 2.70-BeV/c momenta comprise 75% of the total K^- path length. The reactions of interest in this discussion are these:

$$K^- + p \to \Xi^- + K^{+,0} + \pi^{0,+} \quad (1)$$

$$\to \Xi^0 + K^+ + \pi^- \quad (2)$$

$$\to \Lambda^0 + K^0 + \bar{K}^0 \quad (3)$$

$$\to \Lambda^0 + K^+ + K^- \quad (4)$$

$$\to \Sigma^+ + K^0 + K^- \quad (5)$$

$$\to \Sigma^- + K^+ + \bar{K}^0 \quad (6)$$

$$\to \Xi^- + K^{0,+} + \pi^{0,-} + \pi^+ \quad (7)$$

$$\to \Xi^0 + K^0 + \pi^+ + \pi^- \quad (8)$$

$$\to \Xi^- + K^+ + \text{neutrals } (>\pi^0) \quad (9)$$

$$\to \Xi^0 + K^0 + \text{neutrals} \quad (10)$$

$$\to \Lambda^0 + \bar{K}^0 + K^{0,+} + \pi^{0,-} \quad (11)$$

$$\to \Lambda^0 + K^- + K^{0,+} + \pi^{+,0}. \quad (12)$$

We first consider the three kinematically fitted four-body final states of (7) and (8), $\Xi^- K^+ \pi^- \pi^+$, $\Xi^- K^0 \pi^0 \pi^+$, and $\Xi^0 K^0 \pi^+ \pi^-$.[1] Figure 1(a) shows a Dalitz plot of $M^2(\Xi^{-,0}\pi^{\pm})$ versus $M^2(\Xi^{-,0}\pi^{\mp})$ for the $\Xi^- K^+ \pi^- \pi^+$ and $\Xi^0 K^0 \pi^+ \pi^-$ final states. These two have been grouped together, since each reaction has only one $\Xi\pi$ pair in the $t_Z = \pm\frac{1}{2}$ state. We see that both final states are dominated by the $\Xi_{1/2}^*(1530\text{ MeV})$.[2] The pure $T = \frac{3}{2}$ system ($\Xi^-\pi^- + \Xi^0\pi^+$) shows no particular structure.[3] In Fig. 1(b) we have plotted $M^2(\Xi^-\pi^+)$ versus $M^2(\Xi^-\pi^0)$ for $\Xi^- K^0 \pi^0 \pi^+$. In this case, both $\Xi\pi$ systems have $t_Z = \pm\frac{1}{2}$; two orthogonal bands centered at 1530 MeV are evident on this plot. We conclude that the combined three final states involve the production of $\Xi^*(1530)$ in approximately

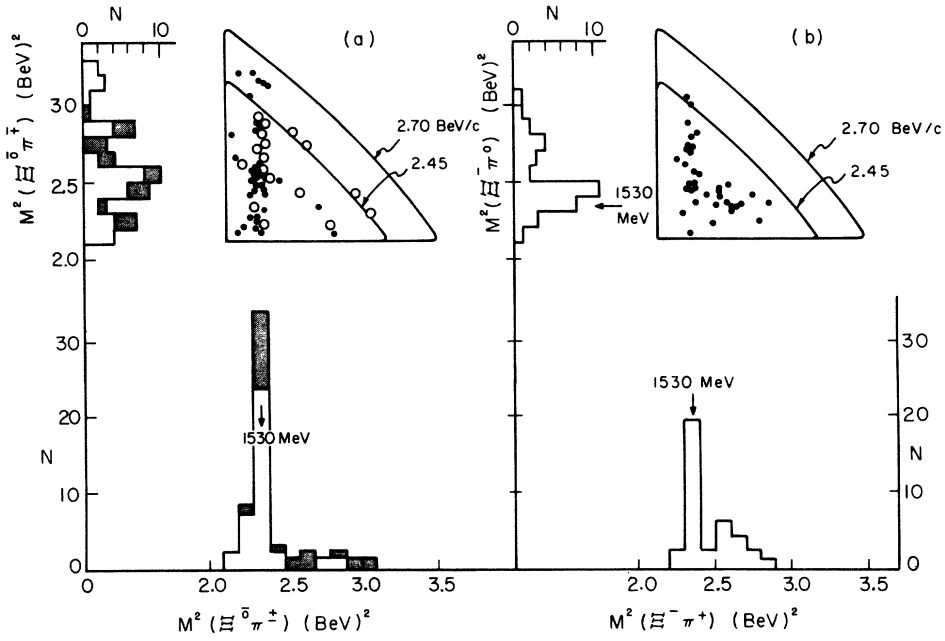

FIG. 1. (a) Dalitz plot of $M^2(\Xi^-,^0\pi^\pm)$ versus $M^2(\Xi^-,^0\pi^\mp)$ for the final states $\Xi^-K^+\pi^-\pi^+$ (solid circles) and $\Xi^0K^0\pi^+\pi^-$ (open circles). In the projections the $\Xi^0K^0\pi^+\pi^-$ events are shaded. (b) Dalitz plot of $M^2(\Xi^-\pi^+)$ versus $M^2(\Xi^-\pi^0)$ for the final state $\Xi^-K^0\pi^0\pi^+$.

70% of the cases.

Considering now the possibility of a $\Xi\pi\pi$ interaction, we turn to Fig. 2, where we have constructed Dalitz plots of $M^2(\Xi\pi\pi)$ versus $M^2(K\pi)$ for the three final states under consideration. Figure 2(a) contains only those events in which a $\Xi^*(1530)$ is produced.[4] Turning our attention to the projection of these events on the $\Xi^*(1530)\pi$ axis, we note an enhancement of events in the 3.1- to 3.4-BeV^2 region. The estimated probability that this peak is due to statistical fluctuation is $\lesssim$1%, based on our best evaluation of the background (upper curve). The Dalitz plot shows a slight clustering of points in the region bounded by $3.1 \leq M^2(\Xi^*(1530)\pi) \leq 3.5$ and $0.76 \leq M^2(K\pi) \leq 0.84$ BeV^2. Since the latter defines a region in which one would expect to observe the $K_{1/2}^*(890 \pm 25$ MeV), this fact could cast some doubt on the validity of a true $\Xi^*\pi$ resonance. However, a detailed evaluation of the relative concentration of various charge states in this region suggests that the clustering of points cannot be explained in a simple manner.[5] In addition, a plot of those events outside the K^* region (unshaded events) still indicates an enhancement in the 3.1- to 3.4-BeV^2 range relative to the apparent background (lower curve). In Fig. 2(b) we present a Dalitz plot for those events that do not satisfy the $\Xi^*(1530)$ selection criteria.[6] Although somewhat limited statistically, the projections give no indication of the structure observed in Fig. 2(a). If we interpret the enhancement in the $\Xi^*(1530)\pi$ projection as a resonance, the best parameters are $E_0 = 1810 \pm 10$ MeV and $\Gamma \sim 70$ MeV.

In Fig. 3 we show the mass distributions of $S = -2$ pairs from three-body final states (1) through (6). In the 1810-MeV region, we note an excess of events in the distribution for $\Lambda^0\overline{K}$ in Fig. 3(b). (We consider for the moment only the shaded area, which is $\Lambda K\overline{K}$ events with the φ removed.) The curve represents our best estimate of the background for these events. Taking this curve at face value, in the 1775- to 1850-MeV interval we observe 55 events when we would expect ~33. Regardless of one's interpretation of the $\Xi^*(1530)\pi$ enhancement, the probability that such a peak is due to a statistical fluctuation is $\lesssim$1%. If one argues that the peaking in $\Lambda^0\overline{K}$ is related to that in $\Xi^*(1530)\pi$, then the odds for such a fluctuation are greatly reduced. To illustrate this point, in Fig. 3(b) we have added the $\Xi^*(1530)\pi$ events of Fig. 2(a) to the shaded area. In the 1775- to 1850-MeV interval we observe 89 events when we expect ~45, giving odds of $\lesssim$0.01% that the enhancement

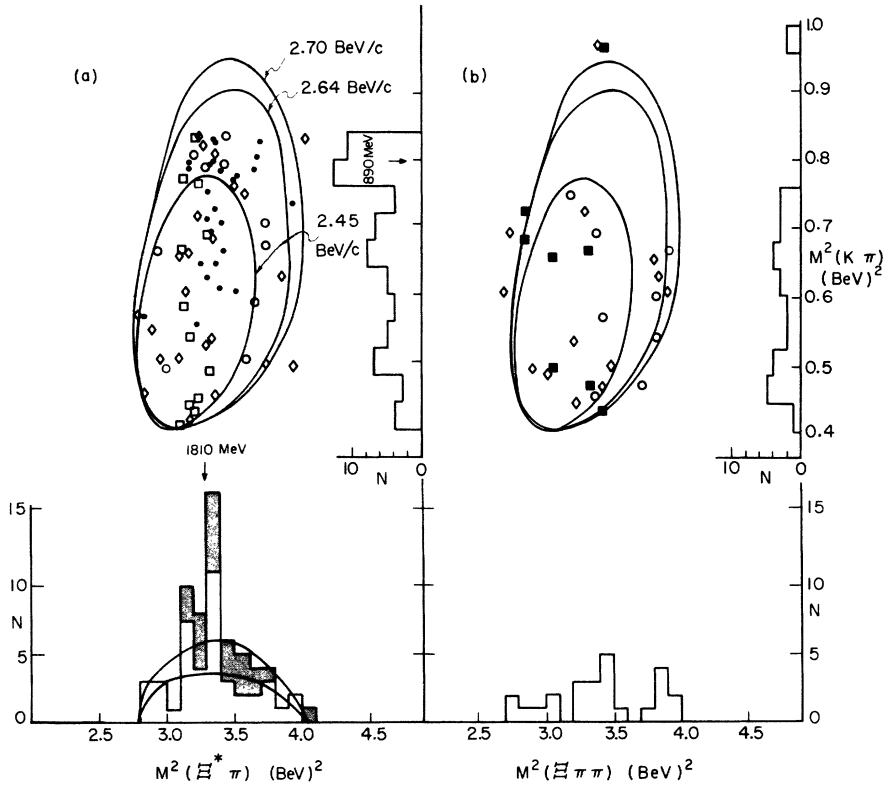

FIG. 2. (a) Dalitz plot of $M^2(\Xi^*(1530)\pi)$ versus $M^2(K\pi)$ for all events containing a $\Xi^*(1530)$. (See reference 4 for criteria used in plotting events.) Final states are denoted by solid circles for $\Xi^-K^0\pi^0\pi^+$, open circles for $\Xi^0K^0\pi^+\pi^-$, and diamonds for $\Xi^-K^+\pi^-\pi^+$. Events in the $\Xi^*(1530)$ overlap region ($\Xi^-K^0\pi^0\pi^+$ only) are plotted twice (squares). The upper curve is the best estimate of the background for all events, the lower is best for those events with the band defined by $0.76 \leq M^2(K\pi) \leq 0.84$ BeV^2 removed (unshaded). (b) Dalitz plot of $M^2(\Xi\pi\pi)$ versus $M^2(K\pi)$ for all events not containing a $\Xi^*(1530)$. (See reference 6.) Final states are denoted by $\Xi^-K^0\pi^0\pi^+$ (squares), $\Xi^0K^0\pi^-\pi^+$ (circles), and $\Xi^-K^+\pi^-\pi^+$ (diamonds).

is a statistical fluctuation. The ~22 events which we ascribe to the 1810-MeV phenomenon in the $\Lambda^0K\overline{K}$ events indicate that the decay rate into $\Lambda^0\overline{K}$ is appreciable.[7] The distributions in $\Xi\pi$ and $\Sigma\overline{K}$ indicate no significant peaking at 1810 MeV. Finally, the (Ξ^-,^{0} + neutrals) and $\Lambda\overline{K}\pi$ systems as derived from events in categories (9) through (12) do not indicate any structure in this region. In the remaining discussion, we consider the 1810-MeV enhancement as seen in $\Xi^*(1530)\pi$ and $\Lambda^0\overline{K}$ as a manifestation of a resonant state, and consider its other properties from this viewpoint.

Isotopic spin.—We consider two reactions, $K^-p \to \Xi^{*0}(1810)K^0$ and $\to \Xi^{*-}(1810)K^+$. Introducing an intermediate decay of the initial $\Xi^*(1810)$ via a state $\Xi_{1/2}^*(1530)+\pi$, we evaluate the branching ratios for $T=\frac{1}{2}$ and $\frac{3}{2}$ assignments of the initial $\Xi^*(1810)$ under the assumption of charge independence in the strong decay. These values, along with experimental counts, are given in Table I. We note that the experimental ratio

$$\left(\Xi^{*0}(1530)\pi^0K^0 \to \Xi^-\pi^+\right) \Big/ \left(\Xi^{*-}(1530)\pi^+K^0 \to \Xi^-\pi^0\right) = 0.7 \pm 0.3$$

is in considerable disagreement with the $T=\frac{3}{2}$ prediction of 4, and one standard deviation removed from the $T=\frac{1}{2}$ prediction of 1.[8] This particular ratio forms a strong test of the isospin, since it is free of scanning bias. The lower-than-expected number of $\Xi^0K^0\pi^+\pi^-$ events (31 ± 6 were expected for $T=\frac{1}{2}$; 18 ± 9 were observed, corrected for neutral decay loss) may be understood in terms of the aforementioned bias, although the statistical uncertainties on these numbers warrant no such explanation. For the $T=\frac{1}{2}$ state, one expects to observe (uncorrected) 2 ± 1 $\Xi^0K^0\pi^0\pi^0$ events and 3 ± 1 $\Xi^-K^+\pi^0\pi^0$ events in the

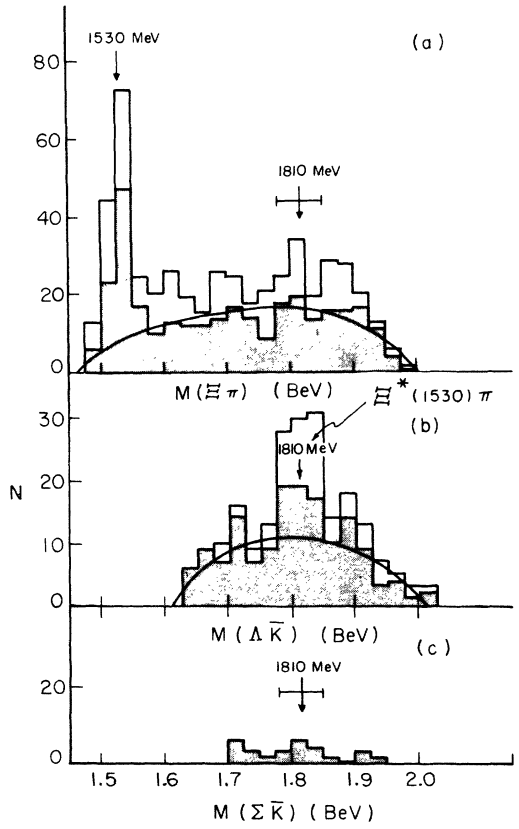

FIG. 3. (a) $\Xi\pi$ mass distribution for combined $\Xi^-K^0\pi^+$, $\Xi^-K^+\pi^0$, and $\Xi^0K^+\pi^-$ final states. Events with an 850- to 950-MeV $K\pi$ mass, corresponding to the $K^*(890)$, have been removed from the shaded events. (b) $\Lambda^0\bar{K}$ mass distribution (shaded area) and $\Xi^*(1530)\pi$ mass distribution from 2(a) (unshaded area). In the shaded region two points for each $\Lambda^0K^0\bar{K}^0$ are plotted since the K^0 and $\bar{K}^0$ are indistinguishable, and one point for each $\Lambda^0K^+K^-$. Events with a 1000- to 1040-MeV mass, corresponding to the φ (1020 MeV), have been removed. (c) $\Sigma\bar{K}$ mass distribution for combined $\Sigma^+K^0K^-$ and $\Sigma^-K^+\bar{K}^0$ final states. Phase-space curves in (a) and (b) are our best estimates of the background distribution for the shaded events.

resonance region (based on 31 ± 6 $\Xi^-\pi^0\pi^+K^0$ events and 20 ± 6 $\Xi^-\pi^+\pi^-K^+$ events, respectively). Both of these numbers are consistent with the absence of any appreciable signal in the ($\Xi^{-,0}$ + neutrals) mass distributions. We conclude that the isospin-$\frac{1}{2}$ assignment for the $\Xi^*(1810)$ is highly favored over $\frac{3}{2}$.[9]

Spin and parity.—Using the $\frac{3}{2}^+$ spin and parity assignment for the $\Xi^*(1530)$,[2,10] we consider spin assignments up to $J=\frac{5}{2}$. For $\frac{1}{2}^+$ and $\frac{3}{2}^+$, the lowest common orbital state for $\Xi^*(1530)\pi$, $\Lambda\bar{K}$, and $\Xi\pi$ is a P wave. The lowest orbital states for $\frac{1}{2}^-$ are D wave for $\Xi^*\pi$ and S wave for $\Lambda\bar{K}$ and $\Xi\pi$. For $\frac{3}{2}^-$ and $\frac{5}{2}^-$, S- and D-wave states respectively are required for $\Xi^*\pi$, with D-wave for both assignments in the case of $\Lambda\bar{K}$ and $\Xi\pi$. The lowest states for $\frac{5}{2}^+$ are P wave for $\Xi^*(1530)\pi$ and F wave for $\Lambda\bar{K}$ and $\Xi\pi$. From simple barrier-penetration arguments,[11] the predicted ratios $\Xi^*(1530)\pi$:$\Lambda\bar{K}$:$\Xi\pi$ are 1:3:3 for $\frac{1}{2}^+$ and $\frac{3}{2}^+$, 1:10:11 for $\frac{1}{2}^-$, 1:0.7:0.9 for $\frac{3}{2}^-$, 1:5:5 for $\frac{5}{2}^-$, and 1:1:1 for $\frac{5}{2}^+$. This approach is clearly highly speculative; however, taken at face value, those spin-parity values that best approximate the experimental results are $\frac{3}{2}^-$ and $\frac{5}{2}^+$. Lastly, we have searched for a possible spin alignment of the resonance by analyzing the strong decay into $\Xi^*(1530)+\pi$. We construct two angles as measured in the rest frame of the $\Xi^*(1810)$—the angles made by the $\Xi^*(1530)$ with respect to (a) the normal to the $\Xi^*(1810)K$ production plane and (b) the line of flight of the $\Xi^*(1810)$ in the K^--p center of mass. The distribution in (a) is consistent with isotropy, suggesting that either the $\Xi^*(1810)$ does not have its spin aligned with respect to the normal, or that the $\Xi^*(1530)\pi$ system is in an $l=0$ orbital state ($J^P=\frac{3}{2}^-$). The distribution in (b) reflects the small anisotropy along the $\Xi^*(1810)$ band of Fig. 2(a), and has been discussed in detail in reference 5.

A group of experimenters using a beam of 3.5-BeV/c K^- in a heavy-liquid bubble chamber have reported the existence of a possible new resonant state of the Ξ with mass ~1770 MeV, width ~80 MeV, and isotopic spin $\frac{1}{2}$.[12] In particular, although low in statistics, their mass distribution for $\Xi^-\pi^+\pi^{0,-}$ combinations in four-body final states demonstrates a peaking in the region of 1700 to 1900 MeV; however, no evidence is presented for a correlation of this peak with the $\Xi^*(1530)$. Their data also suggest, if the effect is related to the $\Xi^*(1810)$, that the $\Xi\pi$ decay mode of $\Xi^*(1810)$ in three-body final states is more abundant relative to the background at 3.5 BeV/c than at lower momenta.

The authors wish to acknowledge the diligent and painstaking effort of the bubble chamber operations group under the direction of Mr. Robert Watt and the scanning and measuring group under the direction of Mr. Edward Hoedemaker. We again thank Professor Luis Alvarez for his continuing interest in this experiment.

*Work done under the auspices of the U. S. Atomic Energy Commission.

[1]Events in the category $\Xi^-K^0\pi^0\pi^+$ are derived from interactions with the topology of a two-prong event with

Table I. Summary of $\Xi K\pi\pi$ final states for initial $T=\frac{1}{2}$ and $\frac{3}{2}$ states of the $\Xi^*(1810)$ decaying through an intermediate system of $\Xi_{1/2}^*(1530)+\pi$.

Reaction	Final state	Clebsch-Gordan coefficients $T=\frac{1}{2}$	Clebsch-Gordan coefficients $T=\frac{3}{2}$	$\Xi^*(1530)$ events in resonance[a] Observed	$\Xi^*(1530)$ events in resonance[a] Corrected[b]
$K^-+p\rightarrow\Xi^{*0}(1810)+K^0$	$\Xi^*(1530)$ ↓				
	$(\Xi^-\pi^0)\pi^+K^0$	$+(2/9)^{1/2}$	$+(1/9)^{1/2}$	$11+6/2$[c]	$(\times 9/7)=18\pm 5$
	$(\Xi^-\pi^+)\pi^0K^0$	$-(2/9)^{1/2}$	$+(4/9)^{1/2}$	$7+6/2$[c]	$(\times 9/7)=13\pm 4$
	$(\Xi^0\pi^-)\pi^+K^0$	$-(4/9)^{1/2}$	$-(2/9)^{1/2}$	3	$(\times 9/2)=14\pm 8$
	$(\Xi^0\pi^0)\pi^0K^0$	$+(1/9)^{1/2}$	$-(2/9)^{1/2}$	~0	$(\times 9/2)$
$K^-+p\rightarrow\Xi^{*-}(1810)+K^+$	$(\Xi^-\pi^0)\pi^0K^+$	$+(1/9)^{1/2}$	$+(2/9)^{1/2}$	~0	$(\times 3/2)$
	$(\Xi^-\pi^+)\pi^-K^+$	$-(4/9)^{1/2}$	$+(2/9)^{1/2}$	13	$(\times 3/2)=20\pm 6$
	$(\Xi^0\pi^-)\pi^0K^+$	$-(2/9)^{1/2}$	$-(4/9)^{1/2}$		$(\times 3/2)$
	$(\Xi^0\pi^0)\pi^-K^+$	$+(2/9)^{1/2}$	$-(1/9)^{1/2}$		$(\times 3/2)$

[a]We define the resonance region to be 1760 through 1860 MeV (~1.5Γ).
[b]Corrections are for neutral decay loss only.
[c]Each event in the 1530-MeV overlap region is counted as one-half event in this tally.

the negative track decaying, plus one vee (K_1^0) or two vees (lambda and K_1^0). The $\Xi^-K^+\pi^-\pi^+$ events used in this discussion appear as a four-prong event with one negative track decaying, plus a vee (lambda). The $\Xi^0K^0\pi^+\pi^-$ events have been restricted to those that appear as a two-prong with two vees (lambda and K_1^0). We have identified 90 events of these types—18 at 2.45 BeV/c, 48 at 2.64 BeV/c, and 24 at 2.70 BeV/c.

[2]For a discussion of the properties of the $\Xi^*(1530)$ see P. L. Connolly, E. L. Hart, G. Kalbfleisch, K. W. Lai, G. London, G. C. Moneti, R. R. Rau, N. P. Samios, I. O. Skillicorn, S. S. Yamamoto, M. Goldberg, M. Gundzik, J. Leitner, and S. Lichtman, Proceedings of the Sienna International Conference on Elementary Particles (Società Italiana di Fisica, Bologna, Italy, 1963); and P. E. Schlein, D. D. Carmony, G. M. Pjerrou, W. E. Slater, D. H. Stork, and H. K. Ticho, Phys. Rev. Letters 11, 167 (1963). We adopt the convention of writing the isospin as a subscript to the state.

[3]The expected density of points on the Dalitz plots of Fig. 1(a) and (b) is nonuniform. The density and the corresponding projections have not been calculated exactly inasmuch as the nature of the final state is so apparent.

[4]The $\Xi^*(1530)$ is defined by $2.3\leq M^2(\Xi^{0,-}\pi^{\pm})\leq 2.4$ BeV^2, and $2.3\leq M^2(\Xi^-\pi^0)\leq 2.5$ BeV^2. The ~60-MeV spread in the 1530-MeV $\Xi^-\pi^0$ peak of Fig. 1(b) is consistent with the calculated resolution for this system as derived from a one-constraint class fit for the reaction $\Xi^-K^0\pi^0\pi^+$. In the case of $\Xi^-K^0\pi^0\pi^+$, the event is accepted if either or both masses satisfy these criteria. The pion common to both axes is that one not included in the $\Xi^*(1530)$. For those events in which only one $\Xi^*(1530)$ is produced, one point is plotted on both the Dalitz plot and the projections. Each event in the $\Xi^*(1530)$ overlap region ($\Xi^-K^0\pi^0\pi^+$ only) is plotted twice on the Dalitz plot and $K\pi$ projection, and once on the $\Xi^*\pi$ projection.

[5]If we assume that a $\Xi^*(1530)K^*(890)$ overlap region does exist on the Dalitz plot, then in this region we expect $[\Xi^{*0}(1530)+K^{*0}(890)\rightarrow K^++\pi^-]/[\Xi^{*0}(1530)+K^{*0}(890)\rightarrow K^0+\pi^0]=2/1$. The experimental ratio is 0.6 ± 0.3 [only for $\Xi^{*0}(1530)\rightarrow\Xi^-+\pi^+$], in considerable contradiction with the prediction. At this time we cannot test $\Xi^{*-}(1530)K^{*+}(890)$ inasmuch as the normalization for the $\Xi^0K^0\pi^+\pi^-$ sample is in doubt.

[6]In this case we always plot the $t_z=\pm\frac{1}{2}K\pi$ combination versus the $\Xi\pi\pi$ combination. We plot two points per event for all $\Xi^-K^0\pi^0\pi^+$ events on the Daltiz plot and the $K\pi$ projection, and one point on the $\Xi\pi\pi$ projection. We note that although the Dalitz envelopes represent the correct kinematic boundaries, the population of events within the boundaries is expected to be nonuniform, with a tendency for peaking at high $\Xi\pi\pi$ mass squared and low $K\pi$ mass squared.

[7]The enhancement in the vicinity of 1810 MeV is particularly strong for those events in which a φ(1020 MeV) is produced. The Dalitz plot of $M^2(K\bar{K})$ versus $M^2(\Lambda^0K$ or $\Lambda^0\bar{K})$ indicates that the simplest explanation of this effect is a spin alignment of the φ along its line of flight in the K^--p center of mass. This results in a $\sin^2\theta$ distribution along the φ band as seen projected on the Λ^0K or $\Lambda^0\bar{K}$ axis. For a discussion of the properties of the φ meson see P. L. Connolly, E. L. Hart, K. W. Lai, G. London, G. C. Moneti, R. R. Rau, N. P. Samios, I. O. Skillicorn, S. S. Yamamoto, M. Goldberg, M. Gundzik, J. Leitner, and S. Lichtman, Proceedings of the Sienna International Conference on Elementary Particles (Società Italiana di Fisica, Bologna, Italy, 1963); and P. Schlein, W. E. Slater, L. T. Smith, D. H. Stork, and H. K. Ticho, Phys. Rev. Letters 10, 368 (1963). However, the non-φ events also exhibit an enhancement in the 1775- to 1850-MeV region. The ~22 events above the curve (primarily $\Lambda^0K^0\bar{K}^0$ because of differences in normalization of the two reactions in this plot) would indicate a branching ratio of about 0.9 for

$$[\Xi^{*0}(1810)\rightarrow\Lambda^0+\bar{K}^0]/[\Xi^{*0}(1810)\rightarrow\Xi^*(1530)+\pi].$$

[8]One may argue that this ratio could be incorrect inasmuch as events in the $\Xi^*(1530)$ overlap region of Fig. 1(b) have been included as well as events that fall in the $K^*(890)$ region of Fig. 2(a). Subtracting these events, we obtain a ratio of 0.4 ± 0.3.

[9]Identification of the $\Lambda\bar{K}$ decay mode as discussed in reference 7 provides a confirmation of this isospin assignment.

[10]The $\frac{3}{2}^+$ assignment for the $\Xi^*(1530)$ is also favored, based on an analysis of $\Xi^*(1530)$ decay by one of us (J. B.-S.). In the following arguments, we assume that the Λ^0 and Ξ are $\frac{1}{2}^+$; the π and K are 0^-.

[11]The angular-momentum and phase-space dependence of the decay rate may be expressed in the form

$$\Gamma \propto |(p^2+X^2)^2|^l (p/m),$$

where p is the momentum of decay products of a resonance of mass M, and X, which is related to the size of the interaction, is adjusted to a size of interaction equal to $\hbar/2m_\pi$. The momenta for $\Xi^*\pi$, $\Lambda\bar{K}$, and $\Xi\pi$ are 230, 390, and 410 MeV/c respectively.

[12]A. Halsteinslid, R. Møllerud, J. M. Olsen, H. H. Bingham, H. Bermeister, D. C. Cundy, G. Myatt, M. Paty, O. Skjeggestad, P. Belliere, V. Brisson, P. Petiau, A. Rousset, C. M. Fisher, J. M. Scarr, F. W. Bullock, and B. S. Luetchford, Proceedings of the Sienna International Conference on Elementary Particles (Società Italiana di Fisica, Bologna, Italy, 1963).

NEW DETERMINATION OF THE MASSES OF Σ^- AND Σ^0 HYPERONS*

R. A. Burnstein, T. B. Day, B. Kehoe, B. Sechi-Zorn, and G. A. Snow
University of Maryland, College Park, Maryland
(Received 8 June 1964)

The low energy K^- beam[1] at the CERN proton synchrotron stopping in the 81-cm Saclay hydrogen bubble chamber[2] yielded many examples of the following at-rest reactions:

$$K^- + p \rightarrow \Sigma^- + \pi^+, \quad (1)$$

$$\Sigma^- + p \rightarrow \Lambda + n, \quad (2)$$

$$\Sigma^- + p \rightarrow \Sigma^0 + n, \quad \Sigma^0 \rightarrow \Lambda + e^+ + e^-. \quad (3)$$

In this note, the mass of the Σ^- hyperon is determined in terms of the better known masses[3] of the other particles in reactions (1) and (2), by measuring the momentum from the range of stopping Σ^- in (1) and from the momentum of the Λ in reaction (2). The (Σ^-, Σ^0) mass difference is determined from the value of the Σ^0 momentum in reaction (3).

A significant experimental error in the Σ^- mass determination arises from the uncertainty of the density of hydrogen in the bubble chamber. The hydrogen density was found by measuring the ranges of a sample of 573 stopping μ^+ from stopping π^+. The mean range of the μ^+ is 1.049 $\pm$ 0.0035 cm (statistical errors only), and corresponds to a hydrogen scale factor of 1.068 $\pm$ 0.0035.[4] Figure 1 shows the μ^+ range distribution. As a further check, we looked at a sample of 400 stopping protons which came from Λ's directly produced from stopping Σ^- via Reaction (2). Using the known mass of the Λ, but treating the Λ momentum and the proton momentum as unknown, we determined the best value for the proton momentum from a two-constraint fit to the Λ decay hypothesis. Comparison of this deduced proton momentum with the measured length of each proton, via the range-momentum table, led to a value of the hydrogen scale factor of 1.068 ± 0.008, in excellent agreement with the value deduced from $\pi^+ \rightarrow \mu^+$ decays. In the analysis that follows we adopt a scale factor of 1.068 ± 0.005.[5]

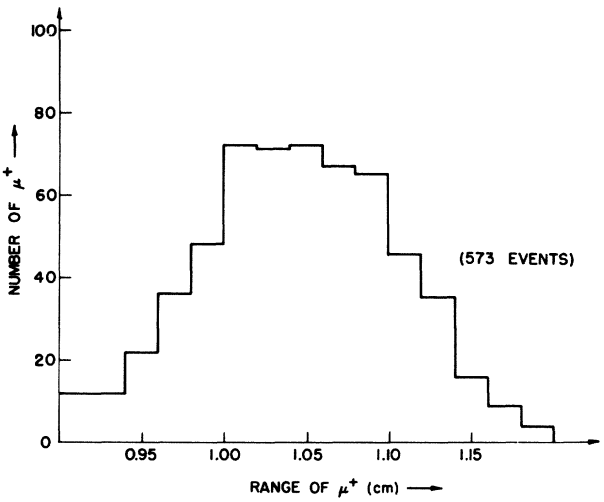

FIG. 1. Observed range distribution of μ^+ from π^+-μ^+ decays at rest.

In addition to the density, the magnetic field in the chamber must be known to a reasonable accuracy.[6] The shape of the magnetic field was de-

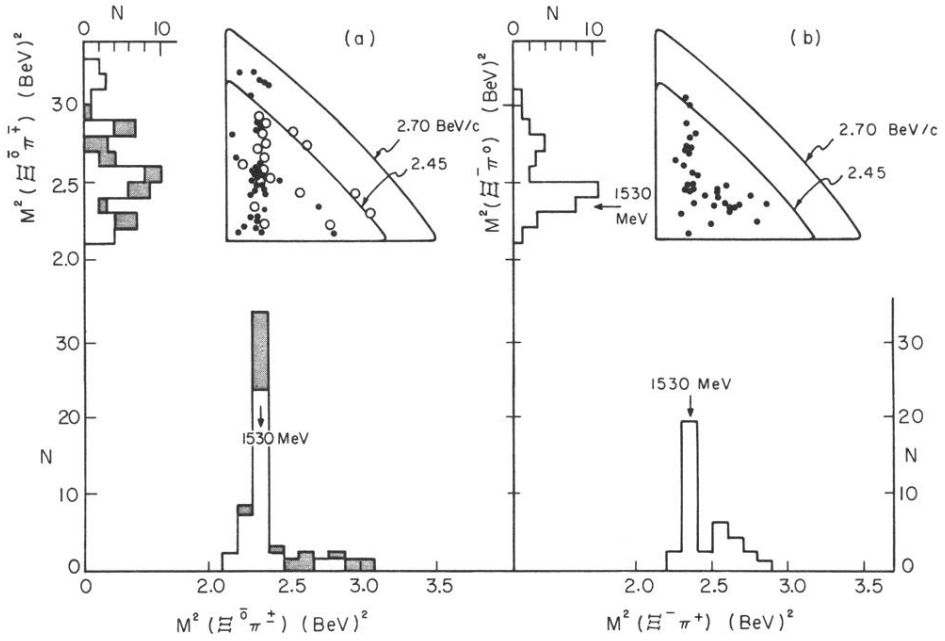

FIG. 1. (a) Dalitz plot of $M^2(\Xi^{-,0}\pi^{\pm})$ versus $M^2(\Xi^{-,0}\pi^{\mp})$ for the final states $\Xi^-K^+\pi^-\pi^+$ (solid circles) and $\Xi^0K^0\pi^+\pi^-$ (open circles). In the projections the $\Xi^0K^0\pi^+\pi^-$ events are shaded. (b) Dalitz plot of $M^2(\Xi^-\pi^+)$ versus $M^2(\Xi^-\pi^0)$ for the final state $\Xi^-K^0\pi^0\pi^+$.

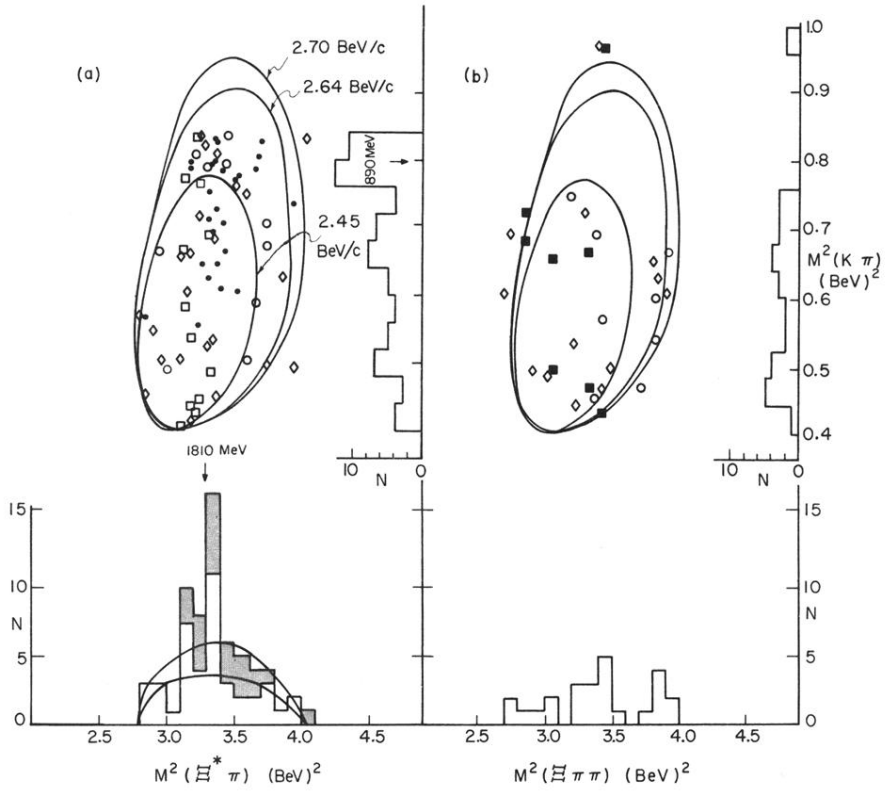

FIG. 2. (a) Dalitz plot of $M^2(\Xi^*(1530)\pi)$ versus $M^2(K\pi)$ for all events containing a $\Xi^*(1530)$. (See reference 4 for criteria used in plotting events.) Final states are denoted by solid circles for $\Xi^-K^0\pi^0\pi^+$, open circles for $\Xi^0K^0\pi^+\pi^-$, and diamonds for $\Xi^-K^+\pi^-\pi^+$. Events in the $\Xi^*(1530)$ overlap region ($\Xi^-K^0\pi^0\pi^+$ only) are plotted twice (squares). The upper curve is the best estimate of the background for all events, the lower is best for those events with the band defined by $0.76 \leq M^2(K\pi) \leq 0.84$ BeV^2 removed (unshaded). (b) Dalitz plot of $M^2(\Xi\pi\pi)$ versus $M^2(K\pi)$ for all events not containing a $\Xi^*(1530)$. (See reference 6.) Final states are denoted by $\Xi^-K^0\pi^0\pi^+$ (squares), $\Xi^0K^0\pi^-\pi^+$ (circles), and $\Xi^-K^+\pi^-\pi^+$ (diamonds).

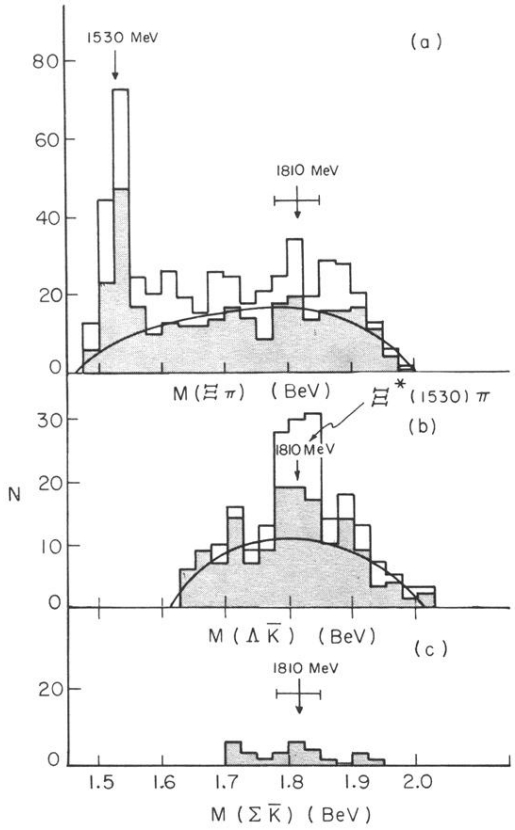

FIG. 3. (a) $\Xi\pi$ mass distribution for combined $\Xi^-K^0\pi^+$, $\Xi^-K^+\pi^0$, and $\Xi^0K^+\pi^-$ final states. Events with an 850- to 950-MeV $K\pi$ mass, corresponding to the $K^*(890)$, have been removed from the shaded events. (b) $\Lambda^0\bar{K}$ mass distribution (shaded area) and $\Xi^*(1530)\pi$ mass distribution from 2(a) (unshaded area). In the shaded region two points for each $\Lambda^0K^0\bar{K}^0$ are plotted since the K^0 and $\bar{K}^0$ are indistinguishable, and one point for each $\Lambda^0K^+K^-$. Events with a 1000- to 1040-MeV mass, corresponding to the φ (1020 MeV), have been removed. (c) $\Sigma\bar{K}$ mass distribution for combined $\Sigma^+K^0K^-$ and $\Sigma^-K^+\bar{K}^0$ final states. Phase-space curves in (a) and (b) are our best estimates of the background distribution for the shaded events.